Study of the Role of Conformation of Thiophene Oligomers on Their Electronic and Magnetic Properties

V. I. Krinichnyi*

Federal Research Center for Problems of Chemical Physics and Medicinal Chemistry, Russian Academy of Sciences, Chernogolovka, Moscow oblast, 142432 Russia
*e-mail: kivi@icp.ac.ru

Abstract—Correlations of electronic and magnetic resonance parameters of spin charge carriers in thiophene oligomers with their polymerization degrees and conformations have been established by comparison of theoretically obtained density functional theory (DFT) and electron paramagnetic resonance (EPR) data with experimental results.

INTRODUCTION

Conjugated organic polymers with an extended $\pi-\pi$ structure are synthesized and studied in many world scientific centers due to the promise of their use as active matrices of efficient and environmentally friendly next-generation electronic, photonic, and spintronic devices with unique electronic properties, such as solar energy converters and batteries, nonlinear optics elements, bandpass filters, fluorescent probes, and sensors [1—3]. Polythiophene (PT) derivatives represented by regioregular poly(3-alkylthiophene) (P3AT) with various side alkyl substituents, e.g., poly(3-hexylthiophene) (P3HT), poly(3-octylthiophene) (P3OT), and poly(3-dodecylthiophene) (P3DDT), are often used as the polymer matrix of such systems. These donor—acceptor compounds are also optimal model systems for establishing the general principles of spin-dependent processes of charge generation, separation, and recombination in many organic polymer devices.

Various methods can be used to study such compounds. For example, detailed information about excited states (excitons) can be obtained by optical polarization dichroism, while high-resolution nuclear magnetic resonance spectroscopy is useful for analyzing some of the anisotropic interactions occurring in these compounds. The fact is that energy transfer in organic polymer systems is carried out by topological distortions, paramagnetic polarons, and/or diamagnetic bipolarons bearing single and double charges, respectively [4]. Polaron pairs in the polythiophene are well separated by radical cations. Partial localization of bipolarons on the PTh chain was discovered

[5], possibly similar to the trapping of charge carriers in other quasi-one-dimensional (Q1D) conjugated systems [6]. The width of polarons and bipolarons in conjugated polymers is usually 3—5 and 5—5.5 polymer units, respectively [7—9].

Most of the processes occurring in systems of this kind depend on the number, relaxation, and dynamics of these charge carriers. This dependence expectedly predetermined the wide use of the direct method of electron paramagnetic resonance (EPR) to establish the detailed parameters of the spin Hamiltonian of polaron radical ions and triplet states upon their doping or photoexcitation, respectively. The method also allows for obtaining more accurate information about the features of electron—electron, electron—nucleus, and electron—phonon interactions; relaxation properties; and the distribution of spin and electron density in these quasi-particles. Despite numerous studies, however, it has not been possible to obtain unambiguous information about the nature of excited states or about the mechanisms of spin—spin interactions and electronic relaxation. The lack of these data is mainly due to different polymer synthesis procedures, stability of polymers, and the specifics of experimental techniques for their study. One of the fundamental features of conjugated aromatic polymers is the possibility of rotation of their units around the principal *x*-axis, which causes the formation of a torsion/dihedral angle between their planes, which is about 150° for polythiophene [10]. This complicates charge transport along this axis. When analyzing the results obtained, it is also necessary to take into account both the possibility of the formation of energetically deep spin traps in

the polymer matrix and their spatial distribution. This necessitates the study of conjugated oligomers using a combination of various experimental and theoretical approaches. The possibility of spatial orientation of an elongated conjugated oligomer by embedding it into a liquid crystal matrix was previously demonstrated [11]. This opens up the possibility of subsequent detailed study of the structural and electronic properties of oligomers and corresponding polymers. Thus, studies of oriented thin films of oligothiophenes with different chain lengths have shown that the main $\pi-\pi^*$ transition is directed parallel to the principal molecular x-axis.

Quantum chemical calculations of the structure and energy parameter of various oligomers were carried out within the framework of density functional theory (DFT) [12]. The bandgap of neutral PTh, E_g, was determined within the framework of the DFT formalism as the difference between the energies of its highest occupied molecular orbital (HOMO) and lowest unoccupied molecular orbital (LUMO), $E_g = E_{LUMO} - E_{HOMO}$, which turned out to be 2.20 eV [13]. The transition of the aromatic PTh isomer to the quinoid one was found to significantly decrease this parameter. The most flexible and at the same time quite effective and simple software package for quantum chemical calculations of the spectroscopic properties of open-shell atomic and molecular systems turned out to be Orca [14] with a wide range of different quantum chemical approaches, including the DFT formalism, as well as direct calculation of the main magnetic resonance parameters of spin charge carriers [15, 16]. Experimental and theoretical studies of a P3DDT-based donor–acceptor system using EPR and DFT methods allowed us to establish a correlation between its photovoltaic efficiency and the bandgap of low-molecular-weight aromatic additives introduced into it [17]. The formation of spin and spinless charge carriers depends on the degree of oxidation. These charge carriers play an important role not only in conjugated organic polymers, but also in other materials. Inorganic semiconductors such as GaAs are well-known examples [18]. Recently, the formation of these charge carriers has also been demonstrated in perovskites of the ABO_3 type [19].

In this work, we performed a detailed comparative DFT and EPR study of the spin-dependent molecular, structural, and magnetic resonance parameters of thiophene oligomers with polaron charge carriers and subsequently correlated them with those experimentally obtained for various Q1D organic semiconductors. For an isolated PTh chain, good agreement between the aforementioned parameters and experiment was found.

METHODS AND PROCEDURES

Structure and Energy DFT Calculations of Thiophene Oligomers

Energy levels of the highest occupied (HOMO) and lowest unoccupied (LUMO) frontier molecular orbitals, E_{HOMO} and E_{LUMO}, as well as the bandgap $E_g = E_{HOMO} - E_{LUMO}$, of thiophene oligomers in aromatic and quinoid conformations with different numbers of monomer units in the absence and presence of polarons with spin $S = 1/2$ and positive elementary charge $+e$ were calculated using the density functional theory (DFT) approximation in the Orca v5.0.4 software environment [14] with the B3LYP functional. The calculations were carried out after preliminary optimization of the geometry of the oligomers using the parallel data transfer (PDT)/message passing interface (MPI) software interface in a multicore processor. The population of electron spins and charge density in the compounds under study were obtained in the Mulliken approximation [20]. Anisotropic spin–spin hyperfine coupling (HFC) constants and the Landé g-factor were determined using the EPRNMR module with the EPRII basis set for nuclei from ^1H to ^{12}C. To take into account ^{32}S atoms, the additional TZVPP basis set was used. To test the effect of the basis set on the calculated EPR parameters, additional single-point calculations were performed using the all-atom def2-TZVPP basis set, which showed minor differences in the calculation of the reported magnetic resonance parameters. Therefore, all calculated parameters presented here were obtained with the EPRII and TZVPP basis sets for all atoms of the oligomers, including the atoms of side substituents and taking into account all possible conformers of the molecular structure. Since no significant influence on the optimized geometry and magnetic resonance parameters was found, all further calculations were carried out under the assumption of vacuum. Band structures and orbital configurations were visualized using the Avogadro v.1.2.0 software [21].

DFT Calculation of EPR Spectra of Polaron Charge Carriers in Thiophene Oligomers

The hyperfine coupling constants and principal g-tensor values of the studied oligomers, obtained in the Orca software package, were used for theoretical simulation and visualization of their high-resolution D-band EPR spectra ($\nu_e = 140$ GHz, $B_0 = 4996$ mT) using the software EasySpin v.5.2 [22]. Taken into account in the simulation of the spectra were their additional anisotropic field-dependent broadening due to unresolved hyperfine splitting, characterized by the tensor (B-strain) [0.039 0.150 0.263] MHz, and the distribution of anisotropic parameters of the spin Hamiltonian described by the tensor (g-strain) [0.0005 0.0004 0.0005]. The calculated EPR spectra

were compared with those obtained experimentally in the millimeter EPR wavelength range.

RESULTS AND DISCUSSION

### Calculation of the Molecular and Band Structure of Thiophene Oligomers

Charge transfer in donor–acceptor elements occurs between the energy levels of the highest occupied molecular orbital (HOMO) and the lowest unoccupied molecular orbital (LUMO). Figure 1a shows the band diagram of neutral polythiophene with molecular energies of HOMO and LUMO, as well as a bandgap designated as E_g^0. Note that the π-atomic orbitals of sulfur, as in the case of nitrogen atoms of polypyrrole [13], should not make a corresponding contribution to the HOMO energy level of polythiophene. In the case of intermolecular electron transfer, for example, in a photovoltaic cell during its illumination, a polaron is formed on the cell chain, carrying spin $S = 1/2$ and charge $+e$. This process is accompanied by the appearance in the bandgap of the polymer matrix of additional energy levels E_1 below the LUMO level and E_2 above the HOMO level (Fig. 2b). If an additional electron enters the polymer chain, a polaron with the opposite orientation relative to the external magnetic field and corresponding energy sublevels is also formed on the latter (Fig. 1c). These parameters, theoretically calculated within the limited Hartree–Fock (LHF) approximation, were E_g^0, E_1, $E_2 = 2.20, 0.71, 0.61$ eV, respectively [13]. The distance between the indicated sublevels depends on the strength of the external magnetic field B_0,

$$\Delta E_{12} = E_g^0 - E_1 - E_2 = 2\mu_B B_0 = \gamma_e \hbar B_0, \qquad (1)$$

where μ_B is the Bohr magneton, γ_e is the gyromagnetic ratio for the electron, and $\hbar = h/2\pi$ is Planck's constant. This value, calculated for EPR studies in the 3-cm and 2-mm ranges using fields of 335.0 and 4887 mT, respectively, is 0.039 and 0.574 meV, respectively.

Distribution of Spin and Charge Densities in Thiophene Oligomers

Figure 2 shows the DFT-optimized structures of 12-mer thiophene oligomers with aromatic and quinoid conformations. The relative values of positive charge density, as well as the electron spin population $S = \frac{1}{2}$, calculated in the Mulliken approximation [20], are given for the corresponding ^1H and ^{32}S atoms of these compounds in Figs. 2a and 2b, respectively. From the data presented, it follows that the potential charge is uniformly distributed on the protons of the neutral and sulfur atoms of the thiophene oligomer, with the exception of the terminal atoms of the end monomer units (see Fig. 2a). It should be noted that
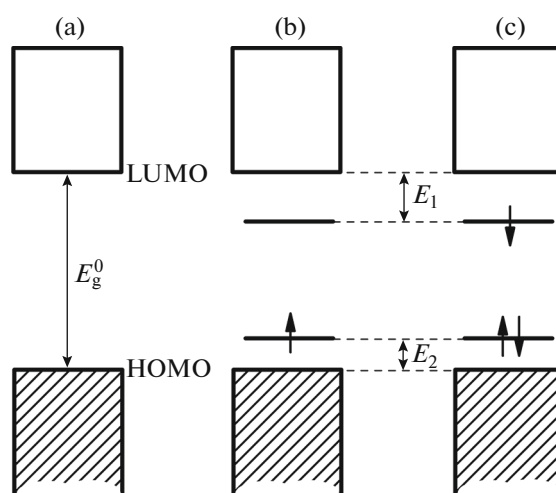

Fig. 1. Evolution of the initial band structure of (a) neutral polythiophene upon elementary-charge |e| leaving its chain, accompanied by the formation of polarons (b) $P^{+\bullet}$ or (c) $P^{-\bullet}$ with the corresponding energy levels E_i in the bandgap.

the charge density on hydrogen atoms is significantly higher, approximately six- to sevenfold, compared to that on sulfur atoms. When a polaron with the quinoid conformation is stabilized on the PTh chain as a result of some influence, this picture changes significantly. This process is accompanied both by the loss of the elementary charge of the polymer system and the appearance of spin polaron (Fig. 2b). In addition, there is a change in the angle of the central monomer from 93.86° in −C−S−C− to 93.76° in =C−S−C=, as well as a decrease in the dihedral/torsion angle S−C=C−S. It is important to note the approximate equality within the polaron of the spin density on sulfur atoms, which differs by more than an order of magnitude from that on hydrogen nuclei. A more detailed picture of changes in the electron and spin populations on each atom of these 12-mer oligothiophene conformers is demonstrated in Fig. 3, in which each data point symbol refers to the corresponding hydrogen, sulfur, or carbon atom constituting the indicated compounds. The presented data show a uniform charge distribution on most PTh atoms. On the other hand, the nature of the spin density distribution clearly indicates the presence in the center of the polaron polymer chain with a characteristic length of about seven monomer units (Figs. 3c, 3f, 3i). This parameter is close to that obtained experimentally for this polymer using the techniques of EPR [8] and electron nuclear double resonance (ENDOR) [23]. Thus, the proposed procedure makes it possible to accurately control the structural, conformational, and magnetic resonance parameters of each atom of the systems under study and other systems based on conjugated organic polymers.
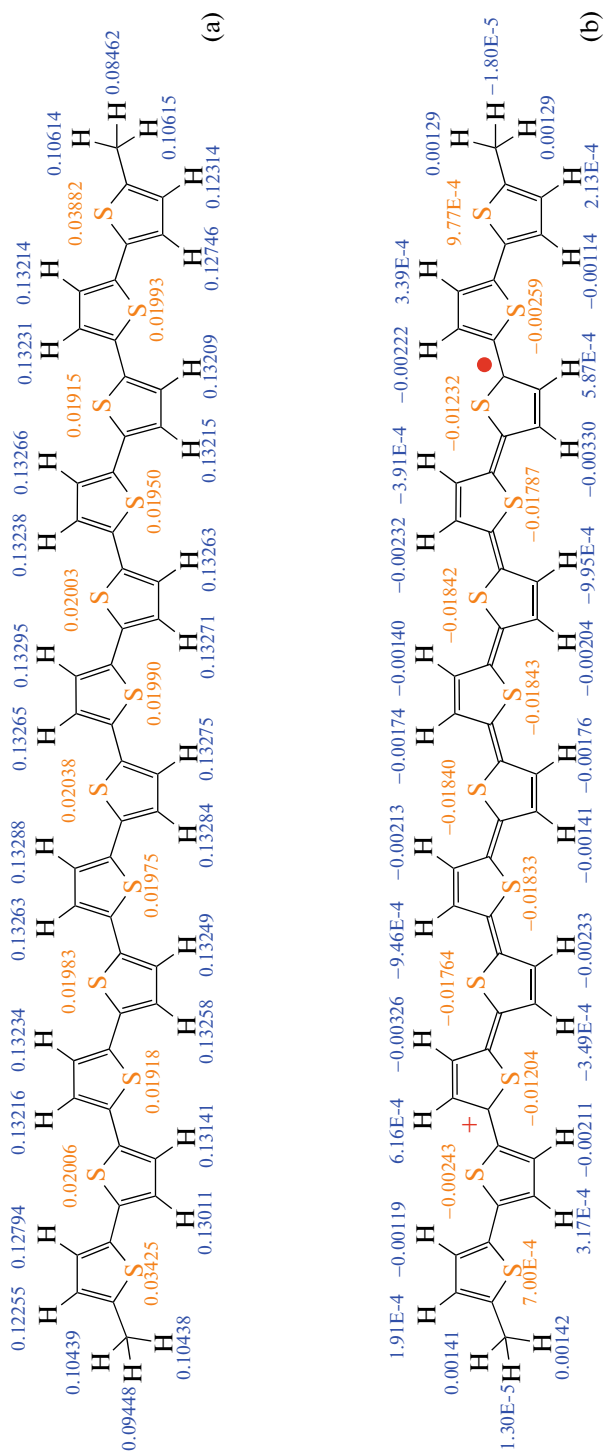
Fig. 2. Density functional theory (DFT) optimized relative (a) charge densities and (b) electron spin densities on hydrogen and sulfur atoms in (a) neutral and (b) oxidized 12-mer thiophene oligomers (PTh) as calculated according to the Mulliken method in the Orca package using the B3LYP functional together with the EPRNMR module and the basis sets EPRII for ¹H and ¹²C atoms and TZVPP for ³²S atoms. Figure 2b shows an eight-unit polaron with the quinoid *trans*-conformation bearing spin $S = \frac{1}{2}$ and an elementary positive charge +*e*. The sums of both densities on all atoms (including ¹²C as well, which is not given here) are equal to (a) zero and (b) unity.
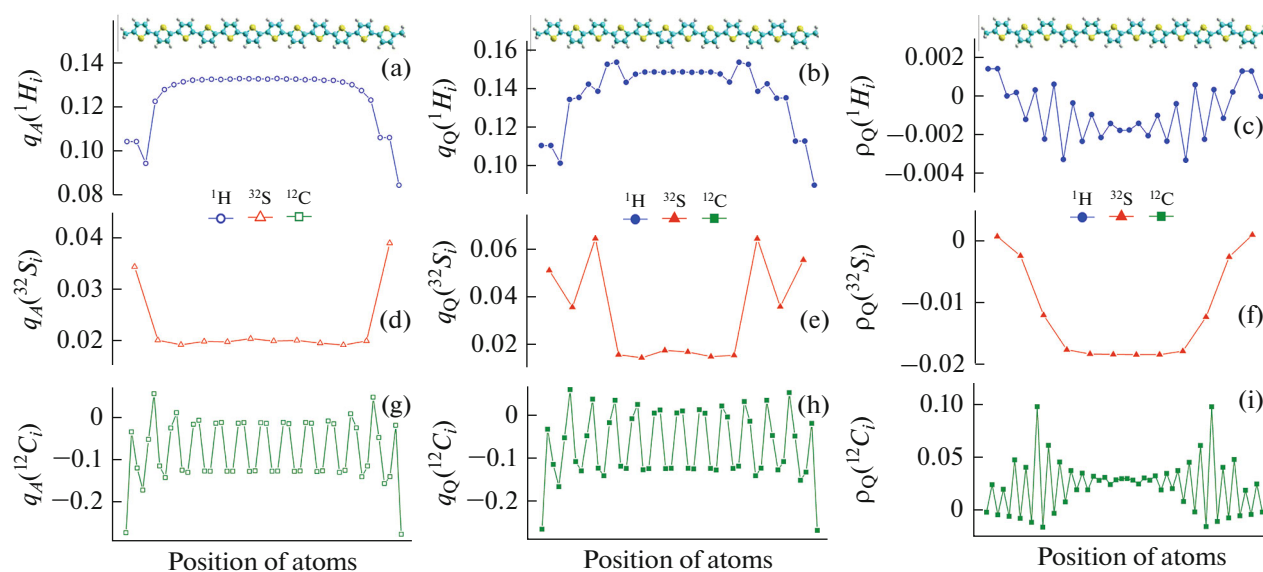
Fig. 3. Changes in (a, b, d, e, g, h) charge densities and (c, f, i) spin densities on the hydrogen (circles), sulfur (triangles), and carbon (squares) nuclei along the main x-axis of the neutral (open symbols) and oxidized (closed symbols) 12-mer thiophene oligomer (schematically shown above), optimized within the density functional theory (DFT) formalism, as calculated using the Mulliken method in the Orca program environment according to the procedure described in the METHODS AND PROCEDURES section.

Calculation of Energy/Band Parameters of Thiophene Oligomers

The energy parameters, HOMO, LUMO, and E_g calculated for neutral and oxidized thiophene oligomers with different numbers of monomers N in the case of polaron spin orientation along and against the direction of the external magnetic field are given in Table 1. The bandgaps determined for these compounds are shown in Fig. 4. As should be expected, the bandgap of the compounds is largely determined by the number of monomer units N and by the spin orientation of polarons generated in them. To a first approximation, these relations can be described by the following exponential law

$$a = a_0 + b \exp(-N/c), \quad (2)$$

where a_0 is the minimum value of the desired parameter for an infinite length of the polymer, i.e. in the limit $N \to \infty$, and b and c are coefficients. It should be noted that other laws making it possible to determine the desired value of a_0 in the limit $N \to \infty$ can be used for this purpose. From the given data it is clear that the upper solid, dashed, and lower solid curves shown in Fig. 4 are indeed well described by Eq. (2) with $a_0 = 2.078$ eV, $b = 5.89$ eV, $c = 1.67$; $a_0 = 2.070$ eV, $b = 5.45$ eV, $c = 1.59$; and $a_0 = 3.153$ eV, $b = 5.03$ eV, $c = 3.15$, respectively. This procedure makes it possible to determine the corresponding bandgap values ($E_g \equiv a_0$) of these and other polymer systems of these compounds. The obtained values turned out to be close to

those calculated for polythiophene (2.20 eV) [13] and estimated experimentally 1.90 [24], 1.92 [25], or 2.07 eV [26] for regioregular P3HT and 1.92 and 1.93 eV for regioregular P3OT and P3DDT, respectively [25].

DFT Calculation of Parameters of the Spin Hamiltonian of Thiophene Oligomers

The analytical tools used in this study also made it possible to calculate the main parameters of the spin Hamiltonian, the HFC constant, as well as the Landé g-factor, which characterize the spin state and interaction of polarons in the studied oligothiophene radical cation. Figure 5 shows the dependences of the averaged/isotropic parameters A_{iso} and g_{iso} of the studied thiophene oligomers of different lengths. The data presented also indicate the dependence of these spin Hamiltonian parameters on the number of monomer units N. These relationships can also be approximated by Eq. (2). Indeed, Fig. 5 demonstrates the exponential dependence of these parameters on the number of monomeric cycles with $a_0 = 0.47$ MHz, $b = 83.62$ MHz, $c = 1.17$ and $a_0 = 2.00162$, $b = 8.71 \times 10^{-4}$, $c = 5.31$, respectively. As in the case of energy parameters, the anisotropic HFC constant and g-factor obtained in the $N \to \infty$ limit for the studied thiophene oligomers were used to calculate the high-resolution D-band EPR spectrum ($\nu_e = 140$ GHz, $B_0 = 4996$ mT) of this compound by means of the EasySpin software package. This spectrum calculated with $A_{iso} =$

Table 1. HOMO and LUMO parameters and E_g (all in eV) for neutral and oxidized thiophene oligomers with different numbers of monomer units N, calculated in the Orca package using the B3LYP functional together with the EPRnmr module and the basis sets EPRII for ^{1}H and ^{12}C atoms and TZVPP for ^{32}S

N	HOMO[a]	LUMO[a]	E_g[a]	HOMO[b]	LUMO[b]	E_g[b]	HOMO[c]	LUMO[c]	E_g[c]
1	−5.513	−0.501	5.012	−11.923	−6.562	5.362	−12.206	−6.288	5.918
2	−4.951	−1.423	3.528	−9.873	−6.136	3.737	−11.223	−8.172	3.051
3	−4.749	−1.851	2.898	−8.870	−5.828	3.042	−9.732	−7.495	2.237
4	−4.655	−2.094	2.561	−8.246	−5.576	2.670	−8.797	−7.070	1.727
5	−4.608	−2.247	2.361	−7.814	−5.367	2.447	−8.159	−6.778	1.381
6	−4.586	−2.349	2.237	−7.494	−5.192	2.302	−7.692	−6.566	1.126
7	−4.577	−2.420	2.157	−7.246	−5.043	2.204	−7.336	−6.406	0.930
8	−4.576	−2.470	2.106	−7.047	−4.911	2.136	−7.053	−6.281	0.772
9	−4.581	−2.507	2.074	−6.882	−4.792	2.090	−6.824	−6.180	0.644
10	−4.588	−2.534	2.054	−6.741	−4.683	2.059	−6.634	−6.096	0.538
11	−4.597	−2.554	2.043	−6.621	−4.582	2.039	−6.476	−6.025	0.451
12	−4.606	−2.569	2.037	−6.582	−4.561	2.021	−6.381	−5.975	0.406

[a] Neutral polymer with the aromatic conformation; [b] polymer in the quinoid conformation with a central polaron having a charge +1 and spin $S = +1/2$, [c] polymer in the quinoid conformation with a central polaron having a charge +1 and spin $S = −1/2$.
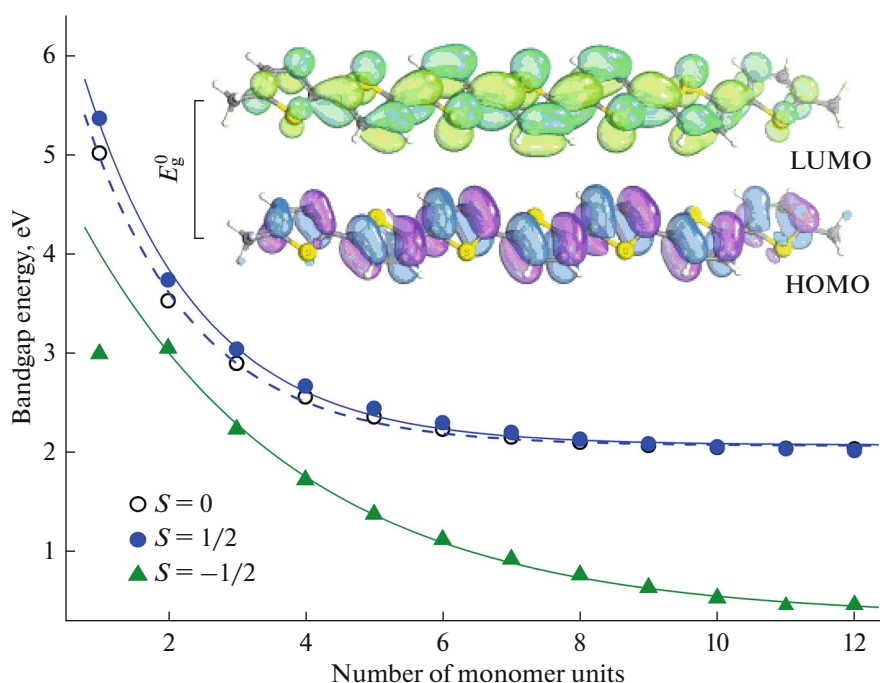
Fig. 4. Change in the bandgap width depending on chain length of DFT-optimized thiophene oligomers, defined as the difference $E_g = E_{HOMO} − E_{LUMO}$ of the corresponding HOMO and LUMO energy levels, calculated in the Mulliken approximation in the Orca package environment according to the procedure, described in the METHODS AND PROCEDURES section. As an example, the upper part shows graphs of isosurfaces of these energy levels calculated for a 7-mer thiophene oligomer. The upper solid, dashed, and lower solid curves show the dependences calculated from Eq. (1) with coefficients $a_0 = 2.078$, $b = 5.89$, $c = 1.67$ eV; $a_0 = 2.070$, $b = 5.45$, $c = 1.59$ eV; and $a_0 = 3.153$, $b = 5.03$, $c = 3.15$ eV, respectively.
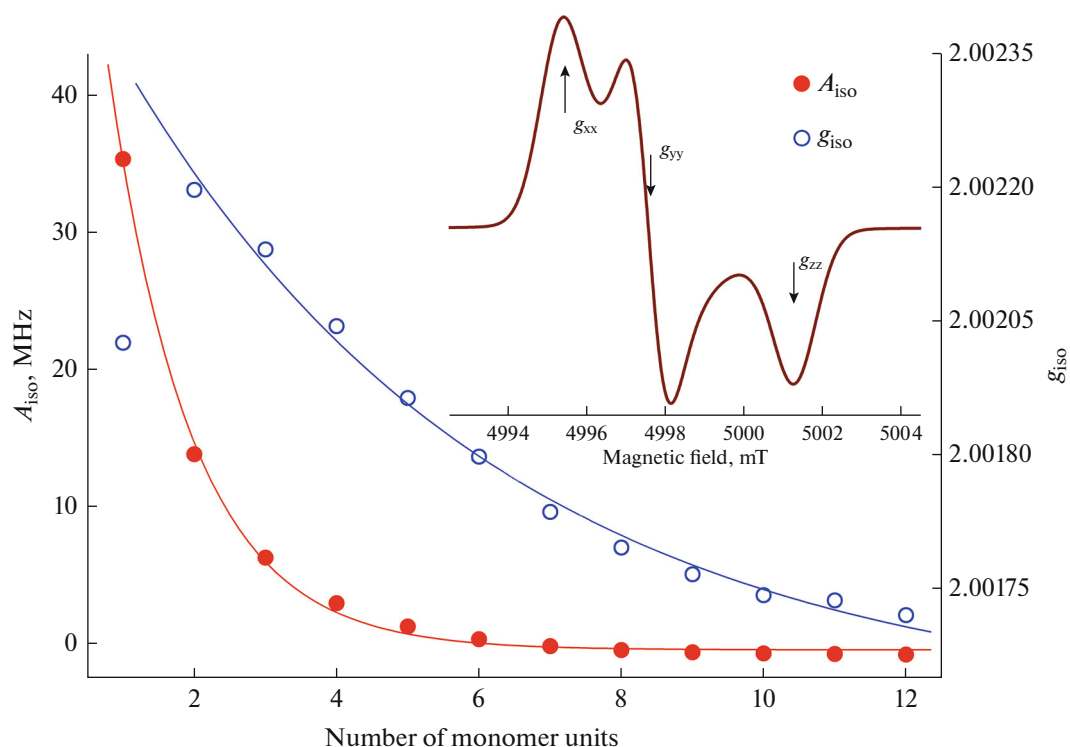
Fig. 5. Dependences of the isotropic spin–spin hyperfine coupling A_{iso} and g-factor g_{iso} of polarons with spin $S = \frac{1}{2}$ and elementary positive charge $+e$ on the thiophene oligomer chain length, as calculated in the Orca package using the B3LYP functional together with module EPRNMR and the basis sets EPRII for ^{1}H and ^{12}C atoms and TZVPP for ^{32}S atoms. The inset shows the 2-mm EPR spectrum calculated for a 12-mer oligothiophene using the EasySpin program and the relevant data given in Table 2. The lower and upper curves were calculated according to Eq. (1) with $a_0 = 0.47$q, $b = 83.62$, $c = 1.17$ and $a_0 = 2.00162$, $b = 8.71 \times 10^{-4}$, $c = 5.31$ MHz, respectively.

Table 2. The principal values of the ^{1}H hyperfine coupling tensors A_i (in MHz); the Landé g-factor of the interaction of polaron spins with an external magnetic field; and their average/isotropic values A_{iso} and g_{iso}, respectively, calculated for oxidized thiophene oligomers with different numbers of monomer units N in the Orca package using the B3LYP functional together with the EPRNMR module and the basis sets EPRII for ^{1}H and ^{12}C atoms and TZVPP for ^{32}S*

N	A_x	A_y	A_z	A_{iso}	g_{xx}	g_{yy}	g_{zz}	g_{iso}
1	34.826	32.965	37.999	35.263	2.001279	2.002066	2.002730	2.002025
2	14.877	12.252	14.206	13.778	2.003815	2.002006	2.000769	2.002197
3	7.172	5.460	6.109	6.247	2.002979	2.002012	2.001398	2.002130
4	4.219	2.028	2.521	2.923	2.003111	2.002021	2.001000	2.002044
5	2.632	0.491	0.562	1.228	2.002906	2.002014	2.000970	2.001963
6	1.704	−0.328	−0.478	0.299	2.002944	2.002007	2.000741	2.001898
7	1.168	−0.743	−1.021	−0.199	2.002857	2.001999	2.000651	2.001836
8	0.819	−0.968	−1.313	−0.487	2.002867	2.001993	2.000528	2.001796
9	0.590	−1.081	−1.451	−0.647	2.002835	2.001975	2.000488	2.001766
10	0.431	−1.133	−1.505	−0.736	2.002854	2.001930	2.000443	2.001742
11	0.332	−1.134	−1.502	−0.768	2.002835	2.001933	2.000443	2.001736
12	0.270	−1.178	−1.524	−0.811	2.00283	2.00191	2.00043	2.001723

* The principal values of the A and g-tensors may not coincide.

0.47 MHz and g_{iso} = 2.00162 is shown in the inset of Fig. 5. The obtained magnetic resonance parameters turned out to be close to those determined experimentally for the virgin and modified polythiophene [16, 27−29].

CONCLUSIONS

The results obtained using the example of polythiophene allow the conclusion that an increase in the planarity of the polymer backbone of this semiconductor and other polymer systems leads to narrowing of the polymer bandgap upon the transition from the aromatic to quinoid PTh conformation, thus expanding the spatial extent of polarons and spin delocalization. A decrease in the dihedral/torsion angle brings planar macromolecules closer together, enhances the hyperfine coupling of their spin charge carriers with their microenvironment, initiates greater delocalization of polarons, and thereby accelerates charge transfer between main chains of a short-chain polymer system. This opens new horizons for controllable functionality of polymer molecular devices with spin-dependent electronic properties.

FUNDING

CONFLICT OF INTEREST

The author of this work declares that he has no conflicts of interest.

REFERENCES

1. *Organic Optoelectronics,* Hu, W., Ed., Weinheim: Wiley−VCH, 2013.
2. Petty, M.C., *Organic and Molecular Electronics: From Principles to Practice*, 2nd ed., Hoboken, NJ: Wiley, 2018.
3. Khalifeh, S., *Polymers in Organic Electronics. Polymer Selection for Electronic, Mechatronic, and Optoelectronic Systems*, Toronto: ChemTec, 2020.
4. Chatterjee, A. and Mukhopadhyay, S., *Polarons and Bipolarons: An Introduction,* Boca Raton, FL: CRC, 2018.
5. Zade, S.S. and Bendikov, M., *J. Phys. Chem. B*, 2006, vol. 110, no. 32, p. 15839.
6. Brazovskii, S.A. and Matveenko, S.I., *J. Exp. Theor. Phys.*, 1992, vol. 192, no. 1, p. 146.
7. Elsenbaumer, R.L. and Shacklette, L.W., *Handbook of Conducting Polymers*, Scotheim, T.E., Ed., New York: Marcel Dekker, 1986, vol. 1, p. 213.
8. Devreux, F., Genoud, F., Nechtschein, M., and Villeret, B., *Springer Series in Solid State Sciences*, vol. 76: *Electronic Properties of Conjugated Polymers*, Kuzmany, H., Mehring, M., and Roth, S., Eds., Berlin: Springer, 1987, p. 270.
9. Westerling, M., Osterbacka, R., and Stubb, H., *Phys. Rev.B: Condens. Matter*, 2002, vol. 66, no. 16, p. 165220.
10. Millefiori, S., Alparone, A., and Millefiori, A., *J. Heterocycl. Chem.*, 2000, vol. 37, p. 847.
11. Sariciftci, N.S., *Synth. Met.*, 1996, vol. 80, no. 2, p. 137.
12. Kohn, W., *Rev. Mod. Phys.*, 1999, vol. 71, no. 5, p. 1253.
13. Brédas, J.L., Themans, B., Fripiat, J.G., Andre, J.M., and Chance, R.R., *Phys. Rev.B: Condens. Matter*, 1084, vol. 29, no. 12, p. 6761.
14. Neeze, F., *Wiley Interdiscip. Rev. Comput. Mol. Sci.*, 2012, vol. 2, no. 1, p. 73.
15. Niklas, J., Mardis, K.L., Banks, B.P., Grooms, G.M., Sperlich, A., Dyakonov, V., Beauprěě, S., Leclerc, M., Xu, T., Yue, L., and Poluektov, O.G., *Phys. Chem. Chem. Phys.*, 2013, vol. 15, no. 24, p. 9562.
16. Van Landeghem, M., Maes, W., Goovaerts, E., and van Doorslaer, S., *J. Magn. Reson.*, 2018, vol. 288, p. 1.
17. Krinichnyi, V.I., Yudanova, E.I., and Denisov, N.N., *J. Phys. Chem. C*, 2022, vol. 126, no. 9, p. 4495.
18. *Springer Series in Materials Science*, vol. 103: *Polarons in Advanced Materials*, Alexandrov, A.S., Ed., Dordrecht: Springer, 2007.
19. Eglitis, R.I., *Int. J. Mod. Phys. B*, 2014, vol. 28, no. 17, p. 1430009.
20. Mulliken, R.S., *J. Chem. Phys.*, 2004, vol. 23, no. 12, p. 2343.
21. Hanwell, M.D., Curtis, D.E., Lonie, D.C., Vandermeersch, T., Zurek, E., and Hutchison, G.R., *J. Cheminformatics*, 2012, vol. 4, no. 1, p. 17.
22. Stoll, S. and Schweiger, A., *J. Magn. Reson.*, 2006, vol. 178, no. 1, pp. 42−55.
23. Kuroda, S., Marumoto, K., Sakanaka, T., Takeuchi, N., Shimoi, Y., Abe, S., Kokubo, H., and Yamamoto, T., *Chem. Phys. Lett.*, 2007, vol. 435, nos. 4−6, p. 273.
24. Kim, D.H., Park, Y.D., Jang, Y.S., Yang, H.C., Kim, Y.H., Han, J.I., Moon, D.G., Park, S.J., Chang, T.Y., Chang, C.W., Joo, M.K., Ryu, C.Y., and Cho, K.W., *Adv. Funct. Mater.*, 2005, vol. 15, no. 1, p. 77.
25. Sensfuss, S. and Al-Ibrahim, M., *Organic Photovoltaics: Mechanisms, Materials, and Devices*, Sun, S.-S. and Sariciftci, N.S., Eds., Boca Raton, FL: CRC, 2005, p. 529.
26. Enengl, C., Enengl, S., Pluczyk, S., Havlicek, M., Lapkowski, M., Neugebauer, H., and Ehrenfreund, E., *ChemPhysChem*, 2016, vol. 17, no. 23, p. 3836.
27. Bernier, P., *Handbook of Conducting Polymers*, Scotheim, T.E., Ed., New York: Marcel Dekker, 1986, vol. 2, p. 1099.
28. Aguirre, A., Gast, P., Orlinskii, S., Akimoto, I., Groenen, E.J.J., El Mkami, H., Goovaerts, E., and van Doorslaer, S., *Phys. Chem. Chem. Phys.*, 2008, vol. 10, no. 47, p. 7129.
29. Konkin, A., Ritter, U., Scharff, P., Roth, H.-K., Aganov, A., Sariciftci, N.S., and Egbe, D.A.M., *Synth. Met.*, 2010, vol. 160, nos. 5−6, p. 485.

Translated by S. Zatonsky